Echo State Networks for Motor Control of Human ECoG Neuroprosthetics

Conference Paper · June 2007

DOI: 10.1109/CNE.2007.369722 · Source: IEEE Xplore

4 authors, including:

Aysegul Gunduz
University of Florida
105 PUBLICATIONS **1,937** CITATIONS
SEE PROFILE

Justin C. Sanchez
DARPA
176 PUBLICATIONS **3,222** CITATIONS
SEE PROFILE

Jose C Principe
University of Florida
1,180 PUBLICATIONS **25,319** CITATIONS
SEE PROFILE

Echo State Networks for Motor Control of Human ECoG Neuroprosthetics

Aysegul Gunduz, Mustafa C. Ozturk, Justin C. Sanchez, and Jose C. Principe

***Abstract*— Towards non-invasive neuroprosthetic systems for motor control, electrocorticogram (ECoG) recordings provide an intermediate step from microwire single neuron recordings to electroencephalograms. Preprocessing modalities that emphasize amplitude modulation and temporal power in the ECoG are employed to build human brain-machine interfaces, which have been previously shown to modulate with hand behavior by means of linear filters, though, with limited accuracy. We improve the online decoding performance of the amplitude modulation across the recording spectra by employing echo state networks (ESNs) which provide nonlinear mappings without compromising training complexity and filter order compared to basic linear filters and other neural networks. Preliminary results show an increase of 15% in the average correlation of ESN outputs with actual hand trajectories compared to linear mappings.**

I. INTRODUCTION

Neuroprosthetics for motor control and brain machine interfaces (BMIs) are areas of research of increasing interest and rapid progress, providing new rehabilitation options to patients who have lost their motor functions due to damage to the nervous system. Regardless of the microscopic or mesoscopic levels of the recordings, the necessity of recordings from multiple sites of the sensorimotor cortex and the multidimensional nature of motor tasks increase the number of parameters involved in the adaptive filter designs which in turn hinders performance and complicates learning.

We have previously proposed preprocessing modalities that emphasize amplitude modulation in mesoscopic electrocorticogram (ECoG) recordings above the level of background noise to model reaching and pointing tasks using linear filters in [1]. Linear filters have well established, low-complexity training methodologies, but may have suboptimal performance since the output is limited to mappings in the input space. The intrinsic neurophysiological mapping of amplitude modulated control features to motor behavior may require nonlinear models. Moreover, for real-time clinical applications, models of low order that are easy to train is desirable. Time delayed neural networks (TDNNs) have been used in BMI experiments and offer a nonlinear mapping; however the number of parameters of the model scales with the embedding of the high dimensional input (32 or greater inputs) thus creating problems with model generalization [2]. To overcome the problem of model order, recurrent neural networks (RNNs) have been tested for BMIs and have produced high accuracy in modeling because they use the advantage of working with the current data samples only and move the memory structure to the hidden, recurrent layer instead of the delayed embedding of TDNN [3].These approaches however, require implementation of the computationally complex backpropagation through time (BPTT).

Introduced by Jaeger, *echo state networks* (ESNs) [4] are RNNs with simplified and efficient learning stages. Indeed, the recurrent connections are all fixed at appropriate values, and only the output weights are trained with least squares, which simplifies tremendously the training. Moreover, by integrating leaky neurons in the ESN structure, the memory depth of the system is increased without increasing filter orders. In this paper, we study and compare mappings from amplitude modulated ECoG features to hand movements involving reaching and pointing tasks using linear filters, echo state networks and leaky echo state networks.

II. MATERIALS AND METHODS

A. Patient

The patient volunteering in this study was undergoing extraoperative subdural grid electroencephalographic monitoring for the treatment of intractable complex partial epilepsy at Shands Hospital, University of Florida. The experimental paradigms were approved by the University of Florida Institutional Review Boards[1]. The patient, a right-handed 15 year old female, underwent a presurgical work-up that included scalp EEG, formal neuropsychological testing, and MRI. The patient's IQ and motor functions were verified to be nonfocal by the absence motor or sensory deficits on neurological examination [1].

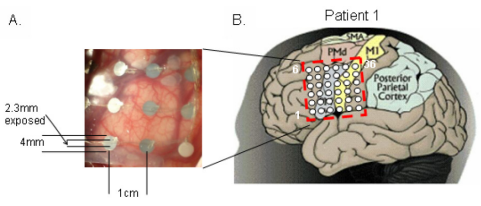

Fig. 1. A. In vivo placement of the electrode grid in a 3x3cm area of cortex and the relative electrode, gyri, sulci, and vasculature relationships. B. Electrode placement

This work was supported in part by DARPA under grant ONR-450595112, the National Science Foundation under Grant #CNS-0540304 and the Children's Miracle Network.

A. Gunduz, M.C. Ozturk and J.C. Principe are with the Computational NeuroEngineering Laboratory at the Department of Electrical and Computer Engineering, University of Florida, Gainesville, FL 32611 (e-mail: {aysegul,can,principe}@cnel.ufl.edu).

J.C. Sanchez is with the Neuroprosthesis Research Group at the Department of Pediatrics, University of Florida, Gainesville, FL 32610 (e-mail: jcs77@ufl.edu).

[1] http://irb.ufl.edu/

The patient was implanted with subdural grid electrodes according to established protocols [5]. The grids consisted of a 1.5mm thick silastic sheet embedded with platinum-iridium electrodes (4mm diameter with 2.3mm diameter exposed surface) spaced at 1-cm center-to-center distances. The anatomical location of the grids was based upon the medical team's recommendation for epilepsy evaluation. The approximate electrode position and numbering as indicated by the surgeon at the time of surgery is presented in Fig. 1. The primary motor cortex was determined by evoked potentials and direct electrical stimulation of the subdural grids [6] and was found to be far from the seizure focus. The 32-channel electrode grid was covering premotor (PMA), primary motor (M1), and somatosensory (S1) cortices based on the patient's cytoarchitecture [1].

B. Experimental Paradigm and Data Collection

Extraction of control features from ECoG recordings for neuroprosthesis is facilitated by continuously time synchronizing neuronal modulation with the well defined behavioral paradigm [1]. The behavioral tasks used in this neuroprosthetic design focus on arm reaching and pointing toward a visual input [1]. The patient was cued to follow with her index finger a predefined cursor trajectory presented on an LCD screen with an active area of (20 x 30cm) while neuronal modulations from the implanted ECoG electrodes were simultaneously being recorded [1]. The trajectory, shown in Fig.2, consisted of a widely performed center-out task and a target selection task. This behavior mimics a computer user's movement to select an icon on the screen. In a single session, the patient was asked to repeat the entire task six times for each trial [1].

Subdural potentials from thirty-two channels were recorded using a Tucker-Davis (Alachua, FL) Pentusa neural recording system at a sampling frequency of 12,207 Hz whilst the patient was engaged in the behavioral task. The sampling rate was determined using the theoretical formulation of the cable equation derived by Nunez [7] which describes the biophysical limits of subdural neural recording (for further details please refer to [1]). The potentials were bandpass filtered from 1Hz to 6kHz while behavioral trajectory recordings were stored with a shared time clock and sampled at 381.5 Hz.

C. Preprocessing: Capturing Amplitude Modulation and Extracting Spectral Bands

Many successful attempts of mapping firing rates of single-unit activities (both linearly and nonlinearly) to behavior can be found in Brain Machine Interface literature many references. Firing rates convert the timing information of action potentials into integrated amplitude modulations [1] by computing the number of action potentials in a bin of size 100msec [8]. Thus, building upon these its strengths, we extract "rate-like" amplitude modulated control features from the ECoG recordings.

The ability to extract spatiotemporal mesoscopic neuronal activation from ECoG electrodes is dependent upon

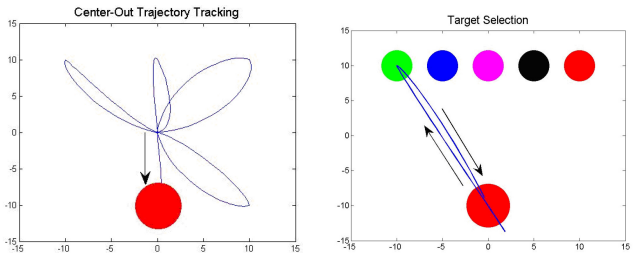

Fig. 2. Behavioral trajectories on a 20x30cm screen

an empirical $1/f^b$ inverse power relation, where $b \approx 2$. Spectrally preprocessed cortical recordings have been shown to correlate with a variety of visual, auditory, and motor tasks in frequency bands comprised of slow potentials (1-60Hz) ,the gamma band (60-100Hz), fast gamma band (100-300Hz) and ensemble depolarization (300-6kHz) [1]. We hypothesize that the amplitude modulations in each band are the result of axonal and dendritic neuronal modulations in the dipoles. Therefore we define the band specific amplitude modulated control features, $u(t)$ as the integrated power of the ECoG voltage $V(t)$ in non-overlapping bins of 100 msec as given in (1):

$$u(t_n) = \sum_{t_i=0}^{100ms} V^2(t_n + t_i), \tag{1}$$

where $t_{n+1} = t_n + 100ms$.

III. ECHO STATE NETWORKS

In BMIs the desired output signal (e.g. hand position) at any given time is modeled a function of the short-term history of the neural signal [8]. Such a dynamical model requires a system with sufficient memory for a proper functional mapping from the neural modulations to the motor output. The simplest of these models is the linear FIR filter, known as the Wiener filter [2], that couples a tap delay line with a linear combiner. Basically, the delay line, which can be thought of as a preprocessor, constructs a sufficiently large state space from the input time series where time is implicit. The optimal output weight matrix, $\mathbf{W}^{linear}$ in the mean square error (MSE) sense can be analytically computed by:

$$\mathbf{W}^{linear} = E[\mathbf{x}\mathbf{x}^T]^{-1} E[\mathbf{x}\mathbf{d}] \tag{2}$$

Here $E[.]$ denotes the expected value operator, $\mathbf{x}$ denotes the input and $\mathbf{d}$ denotes the desired signal.

In neural networks literature, the most common neural architecture for dynamical modeling is the time delay neural network (TDNN) which replaces the linear combiner of the Wiener filter with a static multi-layer perceptron (MLP). The parameters (weights) of the MLP are adapted through the backpropagation algorithm. Both the Wiener filter and the TDNN use a preprocessor to store and access the time history of the input. Recurrent neural networks (RNN) implement a different type of embedding where memory is provided by the feedback created by the recurrent connections between the neurons. One of the main practical problems with RNNs is the difficulty to adapt the system weights. Various algorithms, such as backpropagation through time

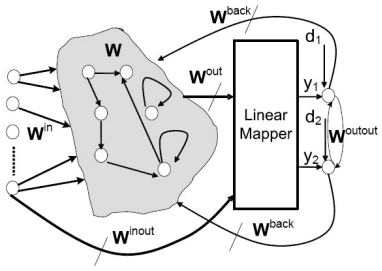

Fig. 3. Block diagram of an Echo State Network

and real-time recurrent learning, have been proposed to train RNNs; however, these algorithms suffer from computational complexity, resulting in slow training, complex performance surfaces, the possibility of instability, and the decay of gradients through the topology and time.

Recently, a new recurrent network paradigm has been proposed by Jaeger [4] under the name of *echo state networks* (ESN) that addresses the difficulties with RNN training. ESNs possess a "large" recurrent topology of nonlinear processing elements (PEs) which constitutes a "reservoir of rich dynamics" [4] and contain information about the history of input or/and output patterns when properly dimensioned. The outputs of these internal PEs (the echo state) are fed to a memoryless but adaptive readout network which is generally linear and reads the reservoir and produces the network output. The interesting property of ESN is that only the memoryless readout is trained, whereas the recurrent topology **W** has fixed connection weights. This reduces the complexity of RNN training to simple linear regression while preserving the recurrent topology.

Fig. 3 depicts an ESN with *M* input channels, *N* internal PEs and *L=2* output units. The value of the input unit at time *n* is $\mathbf{u}(n) = [u_1, u_2(n), ..., u_M(n)]$, of internal PEs are $\mathbf{x}(n) = [x_1, x_2(n), ..., x_N(n)]$, of output units are $\mathbf{y}(n) = [y_1, y_2(n), ..., y_L(n)]$. The connection weights are given in an *N*x*M* weight matrix $\mathbf{W}^{in} = (w_{ij}^{in})$ for connections between the input and the states, in an *N*x*N* matrix $\mathbf{W} = (w_{ij})$ for connections between the PEs, in an *L*x*N* matrix $\mathbf{W}^{out} = (w_{ij}^{out})$ for connections from PEs to the output units, in an *N*x*L* matrix $\mathbf{W}^{back} = (w_{ij}^{back})$ for the connections that project back from the output to the internal PEs, in an *L*x*M* matrix $\mathbf{W}^{inout}$ for connections from input units to output units, and in an *L*x*L* matrix $\mathbf{W}^{outout}$ for connections between output units [4]. Usually, the activation of the internal PEs is updated according to:

$$\mathbf{x}(n+1) = \boldsymbol{f}(\mathbf{W}^{in}\mathbf{u}(n+1) + \mathbf{W}\mathbf{x}(n) + \mathbf{W}^{back}\mathbf{y}(n)) \quad (3)$$

where $\boldsymbol{f} = (f_1, f_2, ..., f_N)$ are the internal unit's activation functions.

Alternatively, each PE can be implemented with a leaky integrator neuron with leakage parameter μ, time constant C, decay rate a and with the update equation:

$$\mathbf{x}(n+1) = (1-\mu Ca)\mathbf{x}(n) + \mu C\boldsymbol{f}(\mathbf{W}^{in}\mathbf{u}(n+1) + \mathbf{W}\mathbf{x}(n) + \mathbf{W}^{back}\mathbf{y}(n)) \quad (4)$$

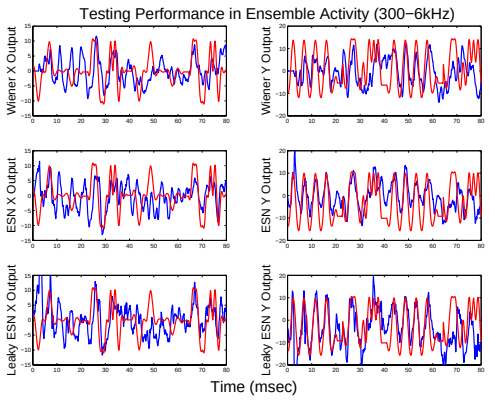

Fig. 4. Results of Wiener, ESN and Leaky ESN in ensemble activity

The leaky neuron implementation basically implements a low-pass filter and is particularly useful when larger memory depths are required. We use the leaky neuron implementation since the ECoG signals change rapidly whereas the desired hand position is at a much slower rate. All f_i's are chosen to be hyperbolic tangent functions, $tanh(.)$. The output from the readout network is computed according to:

$$\mathbf{y}(n+1) = \boldsymbol{f}^{out}(\mathbf{W}^{out}\mathbf{x}(n+1) + \mathbf{W}^{inout}\mathbf{u}(n+1) + \mathbf{W}^{outout}\mathbf{y}(n)) \quad (5)$$

where $\boldsymbol{f}^{out} = (f_1^{out}, f_2^{out}, ..., f_N^{out})$ are the output unit's nonlinear functions. Generally, the readout is linear (i.e. $\boldsymbol{f}^{out}$ is identity). For a linear readout, the optimal output weight matrix, $\mathbf{W}^{out}$ can computed using the Wiener solution.

A basic necessary property for ESN reservoir is the *input forgetting property* which states that for the ESN learning principle to work, the reservoir must asymptotically forget input history. It has been shown in [4] that the input forgetting property is equivalent to s*tate forgetting*, that is, the reservoir must forget its initial state after sufficiently long time. The *echo state condition* can be linked to the spectral radius which is the largest among the absolute values of the eigenvalues of the reservoir's weight matrix, denoted by $||\mathbf{W}||$. This spectral radius has to be less than unity, $||\mathbf{W}|| < 1$. In fact, this condition states that the dynamics of the ESN is uniquely controlled by the input and the effect of initial states vanishes. For the leaky neuron case, it is required that $||\mu C\mathbf{W} + (1-\mu Ca)\mathbf{W}||$ be less than unity, [4].

IV. PERFORMANCE RESULTS

First we map the neuronal modulation to hand movement using a linear Wiener filter topology [2] with 32 channel inputs, 2 output dimensions, and 25 taps. At each time sample, the filter computes the outputs using 2.5 msecs of the past inputs. The model was trained on 3 minutes of recordings and tested on a data segment of 1.5 minutes. The filter order was optimized by scanning tap delays from 5-30 [1].

For the ESN topology the number of processing elements was chosen as $N = 500$. The input weight matrix W_{in} (of size 32-by-500) was fully connected and took on values

TABLE I

TESTING PERFORMANCE

Frequency Bands	Wiener Filter		ESN		Leaky ESN	
	X-pos CC	Y-pos CC	X-pos CC	Y-pos CC	X-pos CC	Y-pos CC
1-60 Hz	0.33 ± 0.16	0.41 ± 0.25	0.39 ± 0.26	0.43 ± 0.26	0.41 ± 0.25	0.44 ± 0.26
60-100 Hz	0.35 ± 0.24	0.41 ± 0.22	0.37 ± 0.25	0.39 ± 0.23	0.43 ± 0.25	0.45 ± 0.26
100-300 Hz	0.34 ± 0.21	0.35 ± 0.25	0.33 ± 0.22	0.50 ± 0.27	0.36 ± 0.26	0.52 ± 0.27
300-6 kHz	0.39 ± 0.26	0.48 ± 0.27	0.50 ± 0.27	0.61 ± 0.29	0.49 ± 0.26	0.63 ± 0.28

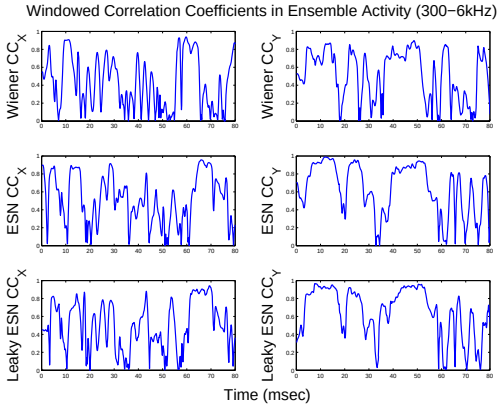

Fig. 5. Windowed correlation coefficients in ensemble activity

of ± 1 with equal probability. The recurrent connection matrix $\mathbf{W}$ was fully connected whose 95% consisted of zero weights. Output feedback and the direct connection from inputs to the output mapper were disconnected (i.e., $\mathbf{W}^{back}, \mathbf{W}^{inout}, \mathbf{W}^{outout}$ were all set to zero). A spectral radius of 0.9 was optimally chosen. For the Leaky ESN system, the number of processing elements were reduced to $N = 200$ due to overtraining in the slow, gamma and high gamma bands. The spectral radius was kept at 0.9 and the leakage parameters a, C, μ were optimized to each band. In both architectures one second of data was discarded as transients. The outputs of the topologies for the x- and y-coordinates for the ensemble activities (300-6kHz) are given in Fig. 4. Averaged correlation coefficients (CC) between the actual hand trajectory and the filter outputs computed over non-overlapping windows of 5 secs for all frequency bands are presented in Table 1. The performance of each model dropped when the patient was switching between tasks. The performance along the y-direction is evidently better for all topologies and all frequency bands compared to x-direction. Across spectral bands the most accurate reconstruction was observed in the ensemble activity (300-6kHz). Overall, the Leaky ESN performed better than the basic ESN and Wiener filter, increasing the CC performance of the Wiener filter by 15% in the y-direction of the 300-6kHz band. Improvement in results with ESNs compared to the linear filter decreased as the input spectral activity slowed down. This may be an indication that the slower frequency bands contribute less to the modulation of hand kinematics.

V. DISCUSSION

In this study we presented real-time neuroprosthesis design for hand motor control that offers a nonlinear, recurrent topology with low training complexity and model order. The ESN topology chosen effectively mapped the ECoG data into a high dimensional space where the filtering and memory retained of the data could be defined by the choice of spectral radius. In this application, the reservoir has the potential to project the ECoG data in such a way that noise is projected in a different part of the space from the neural modulations of interest. Compared to the linear filters, the improvements in the output trajectories of the ESNs were demonstrated as smoother trajectories. Compared to the intrinsic variability of the raw ECoG recordings it is evident that the ESNs are handling the noise sources better than the FIR filtering. The leaky neuron structure further refined the trajectories due to its additional lowpass filtering characteristics. From an implementation point of view, since ESNs only utilize current sample data from channels instead of tap delay lines, the problem of high dimensionality has been overcome. Moreover, this solution did not introduce complexities in training as only the output weights and not the recurrent weights are trained by means of least squares. Additional studies will seek to improve performance of the ESN through optimization of the spectral bands and online selection of input channels.

REFERENCES

[1] J.C. Sanchez, A. Gunduz, J.C. Principe, and P.R. Carney, Extraction and Localization of Mesoscopic Motor Control Signals for Human ECoG Neuroprosthetics, *Journal of Neuroscience Methods*, submitted.

[2] S.P. Kim, J.C. Sanchez, Y.N. Rao, D. Erdogmus, J.C. Principe, J.M. Carmena, M.A. Lebedev, and M.A.L. Nicolelis, A Comparison of Optimal MIMO Linear and Nonlinear Models for Brain-Machine Interfaces, *Journal of Neural Engineering*, vol. 3, pp 145-161, 2006.

[3] J.C. Sanchez, D. Erdogmus, Y. Rao, K.E. Hild, J. Wessberg, M.A.L. Nicolelis, and J.C. Principe, Analysis of the Neural to Motor Representation Space Constructed by a Recurrent Neural Network Trained for a Brain-Machine Interface, *Neural Computation*, submitted, 2005.

[4] H. Jaeger, The "echo state" approach to analyzing and training recurrent neural networks, *GMD-German National Research Institute for Computer Science*, GMD Report 148, 2001.

[5] R.P. Lesser, B. Gordon, R.S. Fisher, E. Vining, and S. Uematsu, Cortical stimulation using subdural electrodes, *Journal of Epilepsy*, vol. 3, pp. 103-106, 1990. H

[6] H. Jasper and W. Penfield, *Epilepsy and the Functional Anatomy of the Human Brain*, Boston: Little, Brown and Co., 1954.

[7] P. L. Nunez and R. Srinivasan, *Electric Fields of the Brain: The Neurophysics of EEG*, New York: Oxford University Press, Second Edition, 2005.

[8] J.C. Sanchez, J.M. Carmena, M.A. Lebedev, M.A.L. Nicolelis, J.G. Harris, and J.. Principe, Ascertaining the importance of neurons to develop better brain machine interfaces, *IEEE Transactions on Biomedical Engineering*, vol. 61, pp. 943-953, 2003.